

C-25 and C-41), 174.8 (s, C-42), 50.6 (q, 42-OMe), 175.3 (s, C-43), 51.6 (q, 43-OMe), 171.3 (s, C-44), and 52.0 (q, 44-OMe); EIMS  $m/z$  761 ( $M^+$ ), 729, 701, and 671.

**8,9-Dihydroxy-43-O-methylmanzamenone A (1c).** To the solution of 43-O-methylmanzamenone A (1a, 26.6 mg, 0.035 mmol) in THF (1.2 mL) and pyridine (0.3 mL) was added 10.5 mg (0.041 mmol) osmium tetroxide in THF (105  $\mu$ L), and the mixture was stirred for 2 h at room temperature. After addition of saturated aqueous sodium bisulfite solution (1.6 mL), stirring was continued for 1 h. Then the mixture was partitioned between ethyl acetate and water. The ethyl acetate layer was dried over sodium sulfate and evaporated under reduced pressure. The residue was purified by a silica gel column with acetone/hexane (1:3) to give the 8,9-diol 1c (27.1 mg):  $^1\text{H NMR}$  ( $\text{CDCl}_3$ )  $\delta_{\text{H}}$  4.08 (1 H, dd,  $J = 7.3$  and 5.8 Hz; H-1), 3.54 (1 H, d,  $J = 5.8$  Hz; H-2), 4.98 (1 H, d,  $J = 4.0$  Hz; H-4), 3.88 (1 H, dd,  $J = 11$  and 4.0 Hz; H-5), 3.61 (1 H, dd,  $J = 11$  and 7.3 Hz; H-6), 1.87 (1 H, m; H-10a), 2.09 (1 H, m; H-10b), 2.41 (1 H, ddd,  $J = 13$ , 9.5, and 5.2 Hz; H-26a), 3.02 (1 H, ddd,  $J = 13$ , 9.5, and 6.3 Hz; H-26b), 1.2-1.6 (56 H, br s; H<sub>2</sub>-11-H<sub>2</sub>-24 and H<sub>2</sub>-27-H<sub>2</sub>-40), 0.88 (6 H, t,  $J = 6.7$  Hz; H<sub>3</sub>-25 and H<sub>3</sub>-41), 3.79, 3.74, and 3.53 (each 3 H, s; 42-OMe, 43-OMe, and 44-OMe);  $^{13}\text{C NMR}$  ( $\text{CDCl}_3$ )  $\delta_{\text{C}}$  42.8 (d, C-1), 45.9 (d, C-2), 132.3 (s, C-3), 125.3 (d, C-4), 41.6 (d, C-5), 44.1 (d, C-6), 93.2 (s, C-8), 91.9 (s, C-9), 39.4 (t, C-10), 31.9, 30.4, 30.3, 29.7 (many carbons overlapped), 27.7, 23.0, and 22.7 (each t, C-11-C-24 and C-26-C-40), 14.1 (2 C, q, C-25 and C-41), 173.2, 172.3, and 164.1 (each s, C-42, C-43, and C-44), 51.9, 51.6, and 51.5 (each q, 42-OMe, 43-OMe, and 44-OMe); FABMS  $m/z$  896 ( $M + \text{diethanolamine} + \text{H}^+$ ), 864, and 846.

**3,4-Dihydroxy-43-O-methylmanzamenone B (2b).** 43-O-Methylmanzamenone B (2a, 6.2 mg, 0.008 mmol) was treated with OsO<sub>4</sub> (2.5 mg, 0.010 mmol) by the same procedure as above to afford the 3,4-diol 2b (1.9 mg):  $^1\text{H NMR}$  ( $\text{CDCl}_3$ )  $\delta_{\text{H}}$  3.66 (1 H, dd,  $J = 11$  and 6.7 Hz; H-1), 2.11 (1 H, d,  $J = 11$  Hz; H-2), 2.48 (1 H, s; 3-OH), 3.70 (1 H, dd,  $J = 6.7$  and 3.0 Hz; H-4), 3.82 (1 H, d,  $J = 3.0$  Hz; 4-OH), 3.25 (1 H, dd,  $J = 11$  and 6.7 Hz; H-5), 3.36 (1 H, t,  $J = 6.7$  Hz; H-6), 1.12 (1 H, m; H-10a), 2.02 (1 H, m; H-10b), 1.93 (1 H, ddd,  $J = 13$ , 9.0, and 5.0 Hz; H-26a), 3.22 (1 H, ddd,  $J = 13$ , 10, and 5.5 Hz; H-26b), 1.2-1.6 (56 H, br s; H<sub>2</sub>-11-H<sub>2</sub>-24 and H<sub>2</sub>-27-H<sub>2</sub>-40), 0.88 (6 H, t,  $J = 6.7$  Hz; H<sub>3</sub>-25 and H<sub>3</sub>-41), 3.77, 3.79, and 3.82 (each 3 H, s; 42-OMe, 43-OMe, and 44-OMe); FABMS  $m/z$  896 ( $M + \text{diethanolamine} + \text{H}^+$ ) and 864.

**Ester Exchange of Manzamenone C (3).** Manzamenone C (3, 0.1 mg) was treated with 2 N HCl/MeOH (0.1 mL) at room temperature for 10 min. After evaporation of the solvent, the residue was analyzed by HPLC [Develosil ODS-5 (5  $\mu$ m, 10  $\times$  250 mm); eluent: MeOH/CHCl<sub>3</sub> (7:3); flow rate: 2.0 mL/min; detection: UV (254 nm)] to show a peak at  $t_{\text{R}}$  20 min together with a small peak at  $t_{\text{R}}$  22 min in the ratio of 8:1, which were ascribed to 43-O-methylmanzamenone A (1a) and the starting material 3, respectively.

**Determination of Amino Acid Residue of Manzamenone E (5).** Manzamenone E (5, 50  $\mu$ g) was heated in 6 N HCl at 110 °C for 24 h. The hydrolyzate was analyzed by a Hitachi amino acid autoanalyzer (Model 835) to show the presence of valine ( $t_{\text{R}}$  55.1 min). For the chiral GC analysis, the acid hydrolysate of manzamenone E (5, 50  $\mu$ m) was treated with 10% HCl/MeOH (0.5 mL) at 100 °C for 30 min. After the reaction mixture was evaporated under vacuum, the residue was heated in a mixture of trifluoroacetic anhydride (0.3 mL) and CH<sub>2</sub>Cl<sub>2</sub> (0.3 mL) at 100 °C for 5 min and then evaporated. The residue was dissolved in CH<sub>2</sub>Cl<sub>2</sub> and subjected to capillary GC analysis [Chirasil-Val column (Alltech, 0.32 mm  $\times$  25 m); carrier gas: nitrogen; program rate: 50-200 °C at 4 °C/min] to show a peak at  $t_{\text{R}}$  6.6 min, which was ascribed to L-valine by comparison with the peaks of TFA/Me derivatives of authentic D- and L-valines ( $t_{\text{R}}$  6.2 and 6.6 min, respectively).

**Ester Exchange of Manzamenone F (6).** Manzamenone F (6, 1 mg) was treated with 2 N HCl/MeOH (5 mL) under reflux for 10 min. After evaporation of the solvent, the residue was analyzed by HPLC [Develosil ODS-5 (5  $\mu$ m, 10  $\times$  250 mm); eluent: CH<sub>3</sub>CN/CHCl<sub>3</sub> (7:3); flow rate: 2.0 mL/min; detection: UV (254 nm)] to show a peak at  $t_{\text{R}}$  32.6 min together with a small peak at  $t_{\text{R}}$  29.0 min in the ratio of ca. 9:1, which were ascribed to 43-O-methylmanzamenone A (1a) and 43-O-methylmanzamenone

B (2a), respectively. The major product 1a was isolated by HPLC (the same conditions as above) and firmly identified by comparison of TLC [ $R_f$  0.45, hexane/EtOAc (3:1)],  $^1\text{H NMR}$ , and EIMS data with those of authentic sample. After reflux for 2 h under the same conditions, the ratio of the products (1a and 2a) was shown to be ca. 1:1 by HPLC analysis.

**3-Carboxy-5-(carboxymethyl)-4-tetradecyl-1-oxacyclopent-3-en-2-one (7):** a colorless oil;  $[\alpha]_{\text{D}}^{25} +12^\circ$  (c 0.78, CHCl<sub>3</sub>); IR (CHCl<sub>3</sub>) 3200, 1740, and 1720  $\text{cm}^{-1}$ ; UV (MeOH)  $\lambda_{\text{max}}$  235 nm ( $\epsilon$  5500);  $^1\text{H NMR}$  ( $\text{CDCl}_3$ )  $\delta_{\text{H}}$  5.24 (1 H, dd,  $J = 8.9$  and 3.6 Hz; H-5), 2.53 (1 H, dd,  $J = 16$  and 8.9 Hz; H-6a), 2.89 (1 H, dd,  $J = 16$  and 3.6 Hz; H-6b), 2.13 (1 H, ddd,  $J = 15$ , 9.0, and 6.0 Hz; H-9a), 2.49 (1 H, ddd,  $J = 15$ , 9.0, and 7.1 Hz; H-9b), 1.2-1.6 (24 H, br s; H<sub>2</sub>-10-H<sub>2</sub>-21), and 0.88 (3 H, t,  $J = 6.9$  Hz; H<sub>3</sub>-22);  $^{13}\text{C NMR}$  ( $\text{CDCl}_3$ )  $\delta_{\text{C}}$  173.4 (s, C-2), 137.7 (s, C-3), 133.8 (s, C-4), 76.8 (d, C-5), 24.5 (t, C-6), 173.4 (s, C-7), 170.0 (s, C-8), 29.7 (many carbons overlapped), 27.1, and 22.7 (each t, C-9-C-21), and 14.1 (q, C-22); EIMS  $m/z$  382 ( $M^+$ ), 338, and 293; HREIMS  $m/z$  382.2372, calcd for C<sub>21</sub>H<sub>34</sub>O<sub>6</sub> (M) 382.2355.

**Dimethyl Ester 7a.** Compound 7 (0.5 mg) in methanol (0.5 mL) was treated with diazomethane in ether (1 mL) at room temperature for 20 min. After evaporation of the solvent, the residue was purified by a silica gel column chromatography (0.5  $\times$  4 cm) with CHCl<sub>3</sub> to afford the dimethyl ester 7a (0.5 mg):  $^1\text{H NMR}$  ( $\text{CDCl}_3$ )  $\delta_{\text{H}}$  5.24 (1 H, dd,  $J = 8.9$  and 3.6 Hz; H-5), 2.53 (1 H, dd,  $J = 16$  and 8.9 Hz; H-6a), 2.89 (1 H, dd,  $J = 16$  and 3.6 Hz; H-6b), 2.13 (1 H, ddd,  $J = 15$ , 9.0, and 6.0 Hz; H-9a), 2.49 (1 H, ddd,  $J = 15$ , 9.0, and 7.1 Hz; H-9b), and 3.74 and 3.95 (each 3 H, s; 7-OMe and 8-OMe), 1.2-1.6 (24 H, br s; H<sub>2</sub>-10-H<sub>2</sub>-21), and 0.88 (3 H, t,  $J = 6.6$  Hz; H<sub>3</sub>-22); EIMS  $m/z$  410 ( $M^+$ ).

**Di-*p*-bromophenacyl Ester (7b).** Compound 7 (2.0 mg) was treated with *p*-bromophenacyl bromide (8.0 mg) in dimethylformamide (0.2 mL) containing potassium fluoride (3.0 mg) at room temperature for 2 h. After addition of H<sub>2</sub>O (0.5 mL), the reaction mixture was extracted with ether (1 mL  $\times$  3). The ether layer was washed with H<sub>2</sub>O (0.5 mL  $\times$  5), dried over sodium sulfate, and evaporated under reduced pressure. The residue was purified by a silica gel column chromatography (1.1  $\times$  4 cm) with hexane/ether (1:1) to give the *p*-bromophenacyl ester 7b (0.6 mg): UV (EtOH)  $\lambda_{\text{max}}$  255 nm ( $\epsilon$  37000); CD (EtOH)  $\lambda_{\text{ext}}$  247 nm ( $\Delta\epsilon +25$ ) and 227 ( $-17$ );  $^1\text{H NMR}$  ( $\text{CDCl}_3$ )  $\delta_{\text{H}}$  5.24 (1 H, dd,  $J = 8.9$  and 3.6 Hz; H-5), 2.72 (1 H, dd,  $J = 16$  and 8.2 Hz; H-6a), 3.06 (1 H, dd,  $J = 16$  and 4.0 Hz; H-6b), 2.23 (1 H, m; H-9a), 2.69 (1 H, m; H-9b), 1.2-1.6 (24 H, br s; H<sub>2</sub>-10-H<sub>2</sub>-21), and 0.88 (3 H, t,  $J = 6.6$  Hz; H<sub>3</sub>-22), 5.27, 5.41, 5.54, and 5.64 (each 1 H, d,  $J = 17$  Hz), 7.61 and 7.64 (each 2 H, d,  $J = 8.3$  Hz), and 7.75 (4 H, d,  $J = 8.3$  Hz); EIMS  $m/z$  776 ( $M^+$ ).

**Acknowledgment.** We thank Mr. Z. Nagahama for his help in collecting the sponge and Drs. J. Fromont and P. R. Bergquist for identification of the sponges.

**Supplementary Material Available:** All spectra of 1a and 7 and  $^1\text{H NMR}$  spectra of manzamenones A-F (1-6) (24 pages). This material is contained in many libraries on microfiche, immediately follows this article in the microfilm version of the journal, and can be ordered from the ACS; see any current masthead page for ordering information.

### Bryostatins Revisited: A New Bryostatins 3 and the Use of NMR To Determine Stereochemistry in the C-20-C-23 Area

Gwendolyn N. Chmurny,\* Mary P. Koleck, and Bruce D. Hilton

PRI/DynCorp Chemical Synthesis and Analysis Laboratory, National Cancer Institute, Frederick Cancer Research and Development Center, P.O. Box B., Frederick, Maryland 21702-1201

Received March 26, 1992

During our continued isolation studies of the bryostatins present in lyophilized *B. neritina*, a new compound, 1, was isolated. It has the same exact mass (by HR FABMS) as

Table I.  $^1\text{H}$  NMR Chemical Shifts<sup>a</sup> of Bryostatin 3 (1), 20-*epi*-Bryostatin 3 (2),<sup>b</sup> Bryostatin 1 (3), and Bryostatin 2 (4)

proton no.	1			2			3			4		
	$\delta$	mult	$J$ (Hz)	$\delta$	mult	$J$ (Hz)	$\delta$	mult	$J$ (Hz)	$\delta$	mult	$J$ (Hz)
190H	5.41	s		5.77	d	1.8	5.15	br s		5.19	bs	
20	5.76	s		5.87	dt	0.6, 1.8	5.18	s		5.20	s	
34	6.08	d	1.8	5.85	t	1.8	6.00 [5.89] <sup>c</sup>	d [d]	1.8 [2.0]	6.01	d	2.0
22ax	4.56	dd	9.0, 1.8	4.47	ddd	9.0, 1.7, 0.6	2.06 [2.09]	m [ddd]	[13.8, 11.3, 2.0]	2.07	ddd	13.8, 11.3, 2.7
22eq							3.69 [3.63]	m [dd]	[13.8, 2.5]	3.69	dd	13.8, 2.3
23	3.75	ddd	11.5, 9.0, 2.5	3.77	ddd	11.4, 9.0, 2.4	4.02 [4.01]	tt [tt]	11.3, 2.4 [11.3, 2.4]	4.02	tt	11.3, 2.5
24a	2.40	ddd	14.2, 12.1, 2.2	2.39	ddd	14.3, 12.3, 2.3	1.83	ddd	13.8, 11.6, 2.9	1.83	ddd	13.9, 11.2, 2.9
24b	1.95	ddd	14.1, 11.4, 2.9	1.88	ddd	14.2, 11.4, 3.1	1.99 [1.99]	m [ddd]	[14.0, 12.5, 2.8]	1.96	ddd	13.9, 12.1, 2.6
25	5.14	ddd	12.2, 5.5, 2.9	5.06	ddd	12.4, 5.5, 3.0	5.17 [5.23]	m [ddd]	[12.2, 4.1, 2.6]	5.19	ddd	12.2, 5.6, 3.0
26	3.76	dq	5.6, 6.4	3.82	dq	5.8, 6.5	3.78 [3.85]	m [dq]	[4.3, 6.5]	3.80	dq	5.6, 6.4

<sup>a</sup>  $\text{CDCl}_3$ , 500 MHz. H-16, H-33, H-40, and H-41 show proton shift differences less than 0.1 ppm. <sup>b</sup> Additional coupling information has been extracted by resolution enhancement or spin simulation. <sup>c</sup> [], recorded in  $\text{CD}_3\text{OD}$ .

Table II.  $^{13}\text{C}$  NMR Chemical Shifts<sup>a</sup> of Bryostatin 3 (1), 20-*epi*-Bryostatin 3 (2), Bryostatin 1 (3), and Bryostatin 2 (4)

carbon no.	$\delta$			
	1	2	3	4
19	99.59	101.65	99.02	99.02
20	69.94	68.57	74.09	74.05
34	117.11	114.31	119.57	119.57
22	79.47	81.23	31.32	31.28
23	70.32	69.08	64.71	64.67
24	33.20	33.19	35.93	35.86
25	72.86	72.91	73.68	73.78
26	69.86	69.70	70.15	70.18

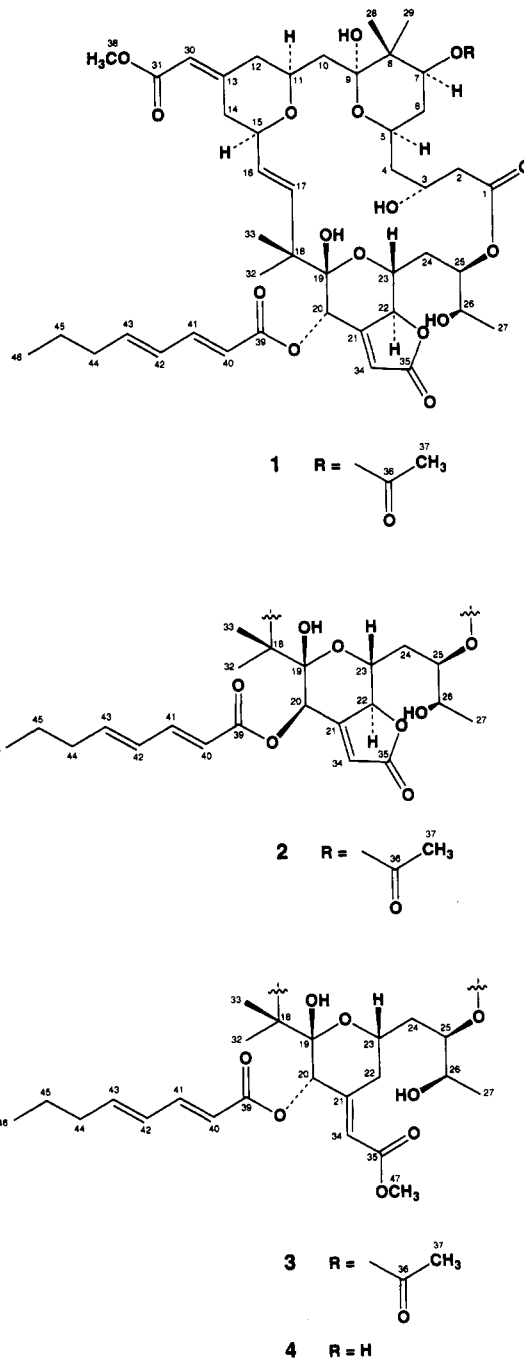
<sup>a</sup>  $\text{CDCl}_3$ , 125 MHz. Carbon atoms 16, 17, 32, and 33 have changes in chemical shifts less than 3 ppm.

a previously isolated bryostatin 3 (2). Compound 2 was erroneously reported by our group<sup>1</sup> to have structure 1 and by Pettit's group<sup>2</sup> to have structure 1 with *cis* geometry between H-22 and H-23. In keeping with the published X-ray structures of bryostatin 1 (3)<sup>3</sup> and bryostatin 2 (4),<sup>2</sup> we have named compound 1 bryostatin 3 and renamed compound 2 20-*epi*-bryostatin 3.

Exhaustive 1D and 2D (TOCSY, DQCOSEY, NOESY, ROESY, HMQC, and HMBC (4 and 8 Hz)) NMR studies of 1 and 2 have established the structures as shown in Figure 1 and provided an NMR technique for distinguishing between isomers at C-20 in other bryostatins. Quantitative 2D NOE studies were necessary to verify the stereochemistry at C-20 and to establish the stereochemistry as *trans* between H-22 and H-23 in both isomers of bryostatin 3.

The one-dimensional  $^1\text{H}$  and  $^{13}\text{C}$  NMR spectra for compounds 1 and 2 differ by no more than 0.05 and 0.5 ppm, respectively, except in the area surrounding C-20. In Tables I and II, 1D NMR comparisons have been given between bryostatin 3 (1), 20-*epi*-bryostatin 3 (2), bryostatin 1 (3),<sup>4</sup> and bryostatin 2 (4) for the area surrounding C-20.

While the proton chemical shift differences in Table I are significant, the coupling data afforded more reliable arguments. In three solvents ( $\text{CDCl}_3$ ,  $\text{C}_3\text{DCN}$ , and  $\text{CD}_3\text{OD}$ ),  $J$  values in the C-20 area were constant, indicating no conformational change; in contrast, chemical shifts changed with solvents and concentration. If the C-20 stereochemistry is bryostatin 1-like, which was established by X-ray,<sup>3</sup> then no spin-spin coupling ( $J$ ) is observed

Figure 1. Structures of bryostatin 3 (1), 20-*epi*-bryostatin 3 (2), bryostatin 1 (3), and bryostatin 2 (4).

between H-34 and H-20, H-20 and 19-OH, and H-20 and H-22. However, if C-20 is epimerized to *epi*-bryostatin

(1) Schaufelberger, D. E.; Chmurny, G. N.; Beutler, J. A. et al. *J. Org. Chem.* 1991, 56, 2895.

(2) Pettit, G. R.; Herald, D. L.; Gao, F. *J. Org. Chem.* 1991, 56, 1337.

(3) Pettit, G. R.; Herald, C. L.; Doubek, D. L. et al. *J. Am. Chem. Soc.* 1982, 104, 6846.

(4) Schaufelberger, D. E.; Chmurny, G. N.; Koleck, M. P. *Magn. Reson. Chem.* 1991, 29, 366.

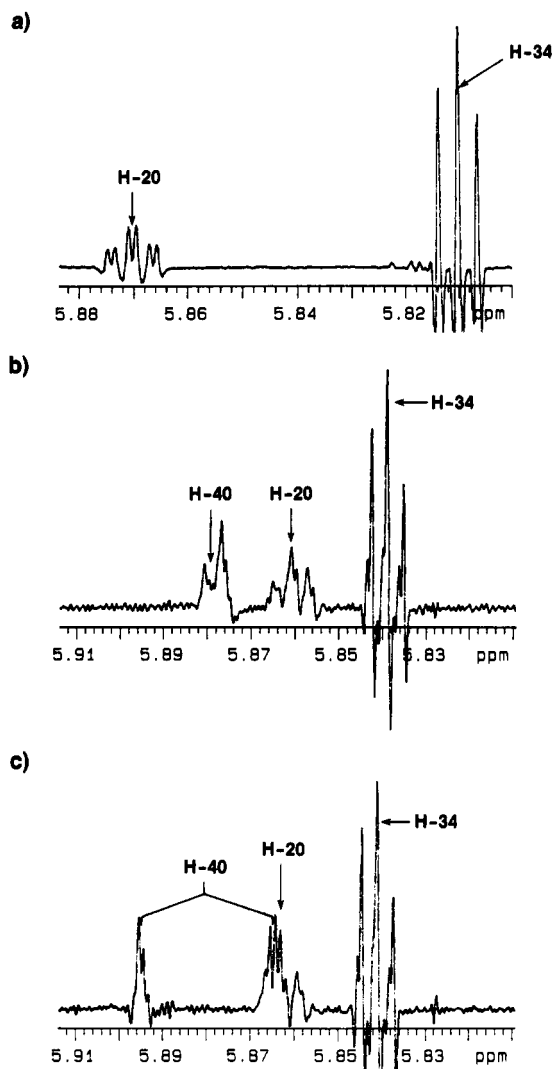


**Figure 2.** 500-MHz proton 1D NMR spectrum of 20-*epi*-bryostatin 3 (**2**) showing H-20 (a) in  $\text{CD}_3\text{CN}$ , (b) in  $\text{CDCl}_3$ , with irradiation of H-41 at 7.39 ppm to reduce the coupling to H-40 and, therefore, to reveal H-20 without overlap (note the Bloch-Siegert shift in resonances), and (c) in  $\text{CDCl}_3$ , without irradiation at H-41.

3-like, then a  $J$  of 1.8 Hz is observed from H-34 to H-20 and H-22, and from H-20 to 19-OH. In this isomer, a smaller " $W^5$ " coupling of 0.6 Hz is also observed from H-20 to H-22 (Figure 2). In  $\text{CDCl}_3$ , H-20 of the *epi* isomer **2** was obscured by half of H-40 as shown in Figure 2c. A reduced-coupling experiment (partial decoupling of H-41, Figure 2b) revealed H-20 clearly. Figure 2a, obtained from the same sample as in Figure 2b and 2c by evaporating the  $\text{CDCl}_3$  and dissolving the sample in  $\text{CD}_3\text{CN}$  showed H-20 clearly with the same "*epi*"-like couplings. Comparison of this  $^1\text{H}$  NMR spectrum in  $\text{CD}_3\text{CN}$  with Pettit's table of NMR shifts established that our 20-*epi*-bryostatin **3** (**2**) is identical to his bryostatin **3**.<sup>2</sup> Quantitative NOE data presented below corroborated the C-20 stereochemistries of **1** and **2**.

The stereochemistry between H-22 and H-23 was shown to be *trans* in both **1** and **2** based on the following evidence. A  $^3J_{\text{HH}}(22,23)$  of 9 Hz in both isomers in  $\text{CD}_3\text{CN}$  as well as in  $\text{CDCl}_3$  indicates a *trans* stereochemistry. The

$^3J_{\text{HH}}(22,23)$  couplings in **3** and **4**, for which both X-ray structures are known, were 11.3 and 2.5 Hz for *trans* (axial-axial) and *cis* (axial-equatorial), respectively. In addition, an average  $^3J_{\text{trans}}$  of 9.5 Hz and  $^3J_{\text{cis}}$  of 2.0 Hz in rapamycin, which has a six-membered ring similar to that in bryostatin **1**, has been reported.<sup>6</sup> Quantitative NOE proton-proton internuclear distances from both C-20 isomers corroborated the *trans* geometry at C-22/C-23, supporting the conclusion that the dihedral angle has not changed.

The ROESY buildup experiment was chosen (see Experimental Section) to provide quantitative internuclear proton-proton distances in  $\text{CDCl}_3$  for **1** and **2** (Table III). The average initial NOE buildup rate from the well resolved methylene pairs on carbon atoms 4, 6, 10, 14, and 24 (Table IIIb) of  $920 \text{ s}^{-1}$  and the average Dreiding model measured H-H distance of 1.8 Å between these  $\text{CH}_2$  pairs were used to quantify NOE buildup rates. For an assumed chair ring, these values tested well on the C-5-C-8 pyran ring (Table IIIc). The reproducibility of the initial buildup rates for proton groups in areas of known geometry in both **1** and **2** gave credence to the data interpretation from ring C-19 to C-23 and H-34. The "anti" H-20/H-22 geometry in **1** resulted in a predicted NOE H-H distance of 4.2 Å (Dreiding model, 3.5 Å), while the "syn" isomer **2** gave 3.3 Å (Dreiding model, 2.67 Å). The relative buildup rates are in agreement with our assignments. The lack of absolute agreement with the Dreiding model and the smaller 9 Hz  $J_{\text{axial-axial}}$  could indicate that this ring is slightly twisted. Although the H-20/H-34 NOE is obscured by chemical shift overlap, it can be seen from Table III that the C-20 stereochemistry is correct. The H-23/19-OH measured distances provided an interesting C-20 stereochemical check. If hydrogen bonding occurs between 19-OH and the ester function of the octadienyl side chain in 20-*epi*-bryostatin **3** (**2**) then the Dreiding model measured H-23-19-OH distance is 2.85 Å, which compares well with the NOE calculated distance of 2.87 Å. In the absence of this hydrogen bonding in bryostatin **3** (**1**), the 19-OH can freely rotate and approach H-23 to within 1.4 Å; the NOE calculated distance was 2.37 Å, which agrees well with the H-23/19-oxygen distance of 2.5 Å (see Table III).

The ROESY buildup rate for H-22/H-23 in both isomers, while negative, corroborates the *trans* geometry about this bond in both **1** and **2**. (Negative rate = same phase as the diagonal; positive rate = opposite phase to the diagonal.) These cross peaks indicate that the NOE does not arise from a direct transverse cross correlation, which would be expected from the *cis* geometry. The H-H distance in the *cis* isomer measured 2.1 Å (Dreiding model) and would be expected to produce a positive ROESY cross peak. The only discrepancy to Pettit's 1D NOE experiment appears to be for H-22/H-23 (for percentages see Table III). We have no explanation except that our 1D H-22/H-23 enhancement in  $\text{CD}_3\text{CN}$  was too small to be reliably observed; this also indicates a *trans* geometry about the H-22/H-23 vicinal bond.

We have established from NMR data that the structures for the two bryostatin **3** isomers are **1**, bryostatin **3**, and **2**, 20-*epi*-bryostatin **3**, and have presented NMR techniques for distinguishing between them. The application of an X-ray determined stereochemistry obtained from a single compound to assign the structures of a presumably homologous series of compounds isolated from the same organisms is commonly used in natural product structure

(5) Jackman, L. M.; Sternhill, S. *Applications of Nuclear Magnetic Resonance Spectroscopy in Organic Chemistry*, 2nd ed.; International Series of Monographs in Organic Chemistry; Pergamon: New York, 1969; Vol. 5, p 334.

(6) Findlay, J. A.; Radics, L. *Can. J. Chem.* 1980, 58, 579.

(7) Macura, S.; Ernst, R. R. *Mol. Phys.* 1980, 41, 95.

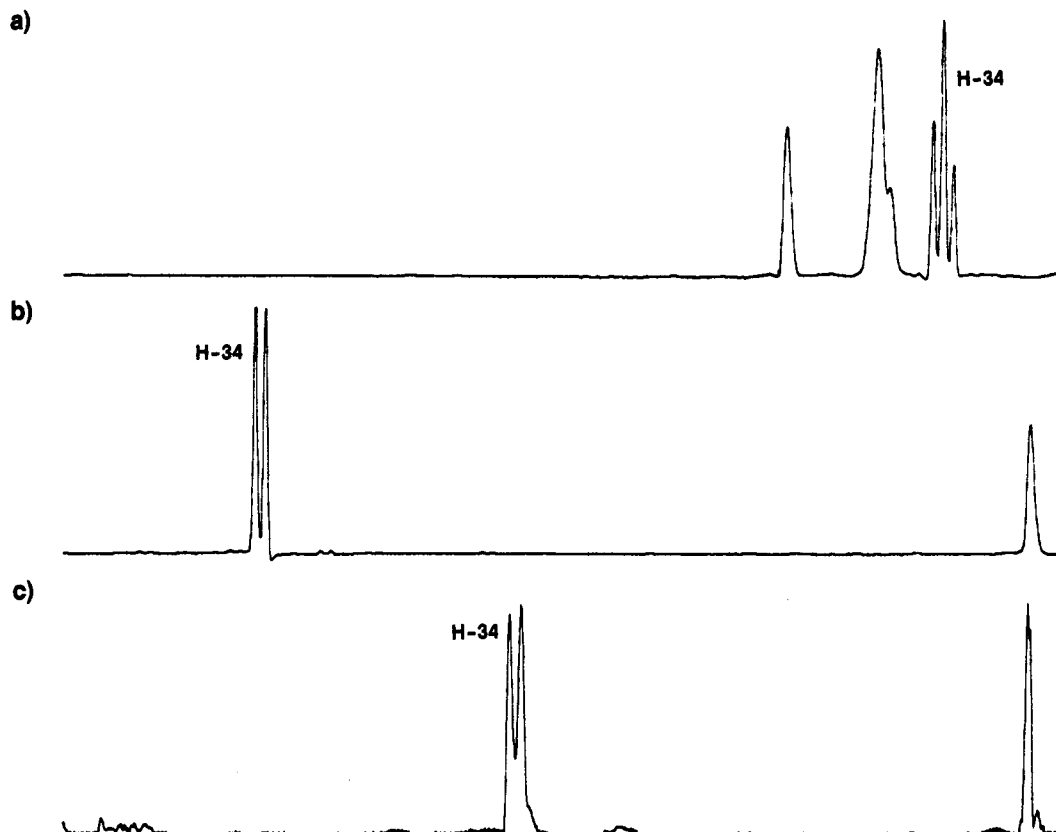


Figure 3. 500-MHz proton 1D NMR spectrum in  $\text{CDCl}_3$  of H-34 in (a) 20-*epi*-bryostatin 3 (2),  $\delta$  5.85, (b) bryostatin 3 (1),  $\delta$  6.08, and (c) bryostatin 1 (3),  $\delta$  6.00.

Table III. 500-MHz ROESY Buildup Data Supporting Structures for Bryostatin 3 (1) and 20-*epi*-Bryostatin 3 (2) in  $\text{CDCl}_3$ , Including Comparisons with 1D NOE Data in  $\text{CD}_3\text{CN}$

	Bryostatin 3 (1)				20- <i>epi</i> Bryostatin 3 (2)				1D NOE enhancement <sup>e</sup>	
	proton-proton interaction	NOE calcd distance <sup>a</sup>	model measured distance <sup>b</sup>	NOE expl rate <sup>c</sup>	calcd rate <sup>d</sup>	NOE calcd distance <sup>a</sup>	model measd distance <sup>b</sup>	NOE expl rate <sup>c</sup>		calcd rate <sup>d</sup>
(a)	20-22	3.5	4.2	17	5.7	2.67	3.3	86	24	3.4, 2.7 <sup>f</sup>
	20-34	2.46	2.7	142	81	<i>g</i>	3.3	<i>g</i>	24	<i>h</i>
	22-23 <sup>i</sup>	-	3.1	-	34	-	3.1	-	37	1.6, - <sup>f</sup>
	23-19 OH	2.37	2.5 <sup>j</sup>	169.3	124	2.87	2.5 <sup>j</sup>	58.8	133	2.4
(b)	4 CH <sub>2</sub>	-	1.8	704 <sup>k</sup>	-	-	1.8	809 <sup>k</sup>	-	-
	6 CH <sub>2</sub>	-	1.8	878 <sup>k</sup>	-	-	1.8	874 <sup>k</sup>	-	-
	10 CH <sub>2</sub>	-	1.8	971 <sup>k</sup>	-	-	1.8	936 <sup>k</sup>	-	-
	14 CH <sub>2</sub>	-	1.8	881 <sup>k</sup>	-	-	1.8	1200 <sup>k</sup>	-	-
	24 CH <sub>2</sub>	-	1.8	1016 <sup>k</sup>	-	-	1.8	979 <sup>k</sup>	-	-
	avg CH <sub>2</sub>	-	1.8	890	-	-	1.8	960	-	-
(c)	5-7	2.25	2.6	234	101	2.31	2.6	217	101	-
	6e-5	2.36	2.5	176	128	2.44	2.5	154	128	-
	6e-7	2.25	2.4	237	163	2.36	2.4	187	163	-
	6a-28	3.22	2.9	40	76 <sup>l</sup>	2.76	2.9	109	76 <sup>l</sup>	-
	7-28	3.22	3.3	40	36 <sup>l</sup>	3.32	3.3	23	36 <sup>l</sup>	-
	7-29	2.53	2.6	186	150 <sup>l</sup>	2.43	2.6	149	150 <sup>l</sup>	-

<sup>a</sup> See text. <sup>b</sup> In Å from a Drieding Model. <sup>c</sup> Initial buildup rates in  $\text{s}^{-1}$ . <sup>d</sup> In  $\text{s}^{-1}$  from Drieding distances. <sup>e</sup> % enhancement = integrated intensity of NOE enhancement/integrated intensity of the saturated peak in NOE difference spectra (in  $\text{CD}_3\text{CN}$ ). <sup>f</sup> Reverse irradiation, i.e., 22/20, 23/22. <sup>g</sup> The close chemical shift  $\Delta\delta = 0.02$  ppm precluded measurement. <sup>h</sup> H20 and H34 are only 0.07 ppm apart and therefore too close to provide reliable 1D NOE measurement. <sup>i</sup> A *cis* geometry predicts a HH distance of 2.1 Å and therefore a strong positive NOE buildup, approximately 356 for 1, 381 for 2. <sup>j</sup> Distance from H23 to 19-oxygen; see text for discussion of H-bonding effect on H23-19OH measured distances. <sup>k</sup> Each rate is an average of the rates from the two cross peaks of a geminal pair in a  $\text{CH}_2$  group. <sup>l</sup> Volume corrected for CH groups<sup>7</sup>. See text. Assumes a chair conformation for the six-membered ring.

elucidation. This was the source of the C-20 stereochemical error reported earlier.<sup>1,2</sup>

### Experimental Section

NMR assignments were made at 500 MHz using the following strategy: (1) integrated proton areas from 1D spectra were assembled by TOCSY connectivities into *J*-coupled groups, (2) these groups were reassembled by COSY connectivities into adjacent

groups, (3) resolution enhanced (line broadening = -1.63; Gaussian apodization = 0.8) 1D spectra and a knowledge from (1) and (2) provided *J*-coupling data, (4) HMQC data and the assigned proton data provided the carbon assignments for protonated carbons, (5) HMBC (8 and 4 Hz) data provided assignments for quaternary carbons, and (6) NOE data and *J* coupling data were used to determine stereochemistry.

ROESY was the technique of choice in molecules of this size for the following reasons: (1) numerous proton spectral overlaps

even at 500 MHz reduce the use of 1D kinetic NOE experiments, (2) because  $\omega\tau_c \approx 1$ , many NOESY cross peaks would be expected to be small or lost entirely, (3) spin diffusion is not as significant in molecules for which  $\tau_c$  is short, and (4) relatively long relaxation times allow for longer linear ROESY buildup observation. The ROESY buildup rates led to more reliable cross-peak volumes, and thus internuclear proton-proton distances because nonlinear buildup rates and peaks opposite in sign to the diagonal ruled out false NOE interactions.

ROESY spectra were obtained nonspinning at 27 °C in CDCl<sub>3</sub> solution using a Kessler spin lock of 30° pulses, States-Haberkmann phase cycling, and arraying the mixing time of the spin lock over the range 50–175 ms. Homospoil irradiation and a recycle delay of 3.4–5 s were employed. From three to six mixing times were used in each experiment. Estimations of initial buildup rates of individual cross peaks were made by volume integration of cross peaks (the integral scale of each spectrum set to a consistent, arbitrary value), and by linear least-squares fit of the volumes versus mixing time to a straight line. Calculation of proton-proton distances were then made under the assumption that the initial buildup rate was proportional to  $r_{ab}^{-6}$  where  $r_{ab}$  is the proton-proton internuclear distance; a fundamental distance reference was obtained by assigning the geminal CH<sub>2</sub> proton-proton distance for all aliphatic CH<sub>2</sub> pairs in the molecule to 1.8 Å.

1D NOE's were obtained in acetonitrile solution by interleaving the collection of spectra in which either an off-resonance or on-resonance presaturation with  $\gamma H_2 \approx 40$  Hz for 3 s was followed with an observed 90° pulse (total recycle delay = 7 s); difference spectroscopy then provided the results.

**Acknowledgment.** The authors wish to thank T. Adams and A. Vatakis for their assistance in the isolation, Dr. C. Metral for providing high-resolution mass spectra, and G. N. McGregor of the Biomedical Supercomputing Center at this facility for writing programs to handle assignments from large 1D and 2D data sets. Research sponsored by the National Cancer Institute, DHHS, under Contract No. N01-CO-74102 with PRI/DynCorp. The content of this publication does not necessarily reflect the views or policies of the Department of Health and Human Services, nor does mention of trade names, commercial products, or organizations imply endorsement by the U.S. Government.

**Supplementary Material Available:** Complete tables of <sup>1</sup>H (500-MHz) and <sup>13</sup>C (125-MHz) NMR assignments in CDCl<sub>3</sub> and IR, UV, and HR FABMS data for bryostatin 3 (1) and 20-*epi*-bryostatin 3 (2) (5 pages). This material is contained in many libraries on microfiche, immediately follows this article in the microfilm version of the journal, and can be ordered from the ACS; see any current masthead page for ordering information.

### New Analogs of *cyclo*(Prn-Prn): Synthesis of Unsymmetric Octahydro-1*H*,5*H*-dipyrrolo[1,2-*a*:1',2'-*d*]pyrazine- 5,10-diones

Mark A. Sanner,\*<sup>†</sup> Carolyn Weigelt,<sup>†</sup> Mary Stansberry,<sup>†</sup>  
Kelly Killeen,<sup>†,1</sup> William F. Michne,<sup>†</sup> Donald W. Kessler,<sup>‡</sup> and  
Rudolph K. Kullig<sup>‡</sup>

Departments of Medicinal Chemistry, Analytical Sciences,  
and Molecular Characterization, Pharmaceuticals Research  
Division, Sterling Winthrop, Inc.,  
Rensselaer, New York 12144

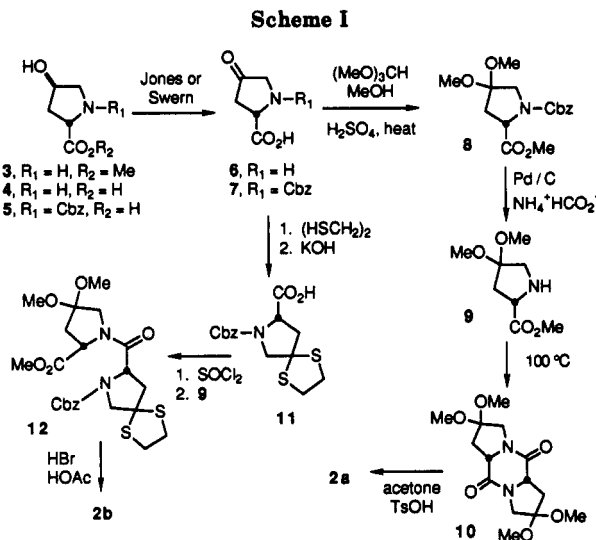
Received February 10, 1992 (Revised Manuscript Received  
June 18, 1992)

Synthesis of *trans*-4-hydroxy-L-proline cyclic dimer (1a,  
*cyclo*(Hyp-Hyp)) was first achieved by Kapfhammer and

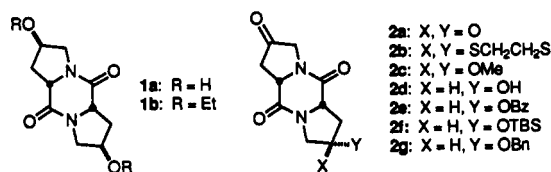
<sup>†</sup> Department of Medicinal Chemistry.

<sup>‡</sup> Department of Analytical Sciences.

<sup>§</sup> Department of Molecular Characterization.



Matthes in 1933 and again in the 1970's by three other groups.<sup>2-6</sup> The only published derivatives of 1a are *O*-ethyl ether 1b and 4-oxo-L-proline cyclic dimer 2a (*cyclo*(Prn-Prn)).<sup>6-9</sup> The highly symmetric, highly functionalized 2a is an inviting framework for constructing conformationally restricted analogs of potential biological interest. In addition to a new preparation of 2a, we report synthetic routes effectively differentiating the homotopic carbonyls and allowing for selective synthesis of congeners masking the C<sub>2</sub> symmetry.



Initially, we anticipated that 2a would provide us with a readily available base of operations for our proposed derivatizations. Although ample supplies of 1a were available by dimerization of *trans*-4-hydroxy-L-proline methyl ester (3),<sup>2</sup> we were unable to consistently reproduce the yield reported for DMSO/DCC oxidation to 2a.<sup>6</sup> Furthermore, the long reaction time (5 days), low solubility of 2a in most organic solvents (1 g/2000 mL of acetone), and the "extensive purification" required with this method discouraged our plans for scale up. A variety of other methods investigated for 1a → 2a conversion including DMSO/(COCl)<sub>2</sub>,<sup>10</sup> DMSO/TFAA, DMSO/SO<sub>3</sub>/pyr, DMSO/DCC/TFA/pyr, Jones reagent,<sup>11</sup> CrO<sub>3</sub>/IRA400/DMF,<sup>12</sup> PCC/DMF, PCC/Al<sub>2</sub>O<sub>3</sub>,<sup>13</sup> and RuO<sub>4</sub><sup>14-16</sup> were

(1) Current address: Department of Chemistry, University of California, Irvine, CA 92717.

(2) Kapfhammer, J.; Matthes, A. *Hoppe-Seyler's Zeit. Physiol. Chem.* 1933, 223, 43.

(3) Eguchi, C.; Kakuta, A. *J. Am. Chem. Soc.* 1974, 96, 3985.

(4) Eguchi, C.; Kakuta, A. *Bull. Chem. Soc. Jpn.* 1974, 47, 2277.

(5) Adams, E. *Int. J. Peptide Prot. Res.* 1976, 8, 503.

(6) Shirota, F. N.; Nagasawa, H. T.; Elberling, J. A. *J. Med. Chem.* 1977, 20, 1176.

(7) Magerlein, B. J. *J. Med. Chem.* 1967, 10, 1161.

(8) Ma, X.; Zhao, Y. *J. Org. Chem.* 1989, 54, 4005.

(9) Witiak, D. T.; Wei, Y. In *Progress in Drug Research*; Jucker, E., Ed.; Birkhäuser Verlag: Basel, 1990; pp 249-363.

(10) Tidwell, T. T. *Synthesis* 1990, 857.

(11) Bowden, K.; Heilbron, I. M.; Jones, E. R. H.; Weedon, B. C. L. *J. Chem. Soc.* 1946, 39.

(12) Cainelli, G.; Cardillo, G.; Orena, M.; Sandri, S. *J. Am. Chem. Soc.* 1976, 98, 6737.

(13) Cheng, Y.-S.; Liu, W.-L.; Chen, S. *Synthesis* 1980, 223.

(14) Caputo, J. A.; Fuchs, R. *Tetrahedron Lett.* 1967, 4729.

(15) Nakata, H. *Tetrahedron* 1963, 19, 1959.